Angiogenesis (2014) 17:77–91
DOI 10.1007/s10456-013-9379-0

ORIGINAL PAPER

The heparan sulfate editing enzyme Sulf1 plays a novel role in zebrafish VegfA mediated arterial venous identity

Bushra Gorsi · Feng Liu · Xing Ma · Timothy J. A. Chico · Ashok Shrinivasan · Kenneth L. Kramer · Esther Bridges · Rui Monteiro · Adrian L. Harris · Roger Patient · Sally E. Stringer

Received: 9 October 2012 / Accepted: 5 August 2013 / Published online: 20 August 2013

Abstract Arterial and venous specification is critical for establishing and maintaining a functioning vascular system, and defects in key arteriovenous signaling pathways including VEGF (vascular endothelial growth factor) lead to congenital arteriopathies. The activities of VEGF, are in part controlled by heparan sulfate (HS) proteoglycans, significant components of the endothelial glycocalyx. The level of 6-O sulfation on HS polysaccharide chains, that mediate the interaction between HS and VEGFA, is edited at the cell surface by the enzyme SULF1. We investigated the role of sulf1 in vascular development. In zebrafish *sulf1* is expressed in the head and tail vasculature, corresponding spatially and temporally with vascular development. Targeted knockdown of *sulf1* by antisense morpholinos resulted in severe vascular patterning and maturation defects. 93 % of *sulf1* morphants show dysmorphogenesis in arterial development leading to occlusion of the distal aorta and lack of axial and cranial circulation. Co-injection of $vegfa_{165}$ mRNA rescued circulatory defects. While the genes affecting haematopoiesis are unchanged, expression of several arterial markers downstream of VegfA signalling such as *notch* and *ephrinB2* are severely reduced in the dorsal aorta, with a concomitant increase in expression of the venous markers *flt4* in the dorsal aorta of the morphants. Furthermore, in vitro, lack of *SULF1* expression downregulates VEGFA-mediated arterial marker expression, confirming that Sulf1 mediates arterial specification by regulating $VegfA_{165}$ activity. This study provides the first in vivo evidence for the integral role of the endothelial glycocalyx in specifying arterial-venous identity, vascular patterning and arterial integrity, and will help to better understand congenital arteriopathies.

Electronic supplementary material The online version of this article (doi:10.1007/s10456-013-9379-0) contains supplementary material, which is available to authorized users.

B. Gorsi (✉)
Cardiovascular Medicine, Faculty of Medical and Human Sciences, University of Manchester, Manchester, UK
e-mail: bgorsi@genetics.utah.edu

Present Address:
B. Gorsi
Department of Neurobiology and Anatomy, Eccles Institute of Human Genetics, University of Utah Molecular Medicine Program, Building 533, Room 3160, 15 North 2030 East, Salt Lake City, UT 84112-5330, USA

F. Liu
State Key Laboratory of Biomembrane and Membrane Biotechnology, Institute of Zoology, Chinese Academy of Sciences, Beijing 100101, China

X. Ma
MRC Centre for Developmental and Biomedical Genetics, University of Sheffield, Sheffield, UK

T. J. A. Chico
Department of Cardiovascular Science, MRC Centre for Developmental and Biomedical Genetics, University of Sheffield, Sheffield, UK

A. Shrinivasan · K. L. Kramer
National Heart, Lung, and Blood Institute, National Institutes of Health, Bethesda, MD, USA

E. Bridges · R. Monteiro · A. L. Harris · R. Patient
Weatherall Institute of Molecular Medicine, University of Oxford, Oxford, UK

S. E. Stringer (✉)
Faculty of Medical and Human Sciences, Institute of Cardiovascular Sciences, University of Manchester, Core Technologies Facility, 46 Grafton Street, Manchester M13 9NT, UK
e-mail: sally.stringer@manchester.ac.uk

Keywords Angiogenesis · Arteries · VEGF · Glycocalyx · Sulf1

Introduction

Molecular distinction between arteries and veins is one of the early events of vascular development, that leads to the expression of specific arterial and venous markers such as *ephrinB2a* and *ephB4* respectively [1]. Genetic loss of arterial vs venous specification leads to arteriovenous (A-V) malformations including A-V shunts that are characteristic of congenital arteriopathies such as hereditary hemorrhagic telangiectasia (HTT) [2, 3]. Vascular endothelial growth factor (VEGF) plays a central role in arterial specification and differentiation, as well as being critical for the function and maintenance of vascular endothelium [4]. The role of VEGF in many aspects of blood vessel formation is well characterized, including proliferation, migration of endothelial cells and as a vascular permeability factor [5]. Experimental evidence in zebrafish has shown VegfA to have a crucial role in arterial differentiation [6]. Loss of Hedgehog signaling (*shh)* leads to downregulation of VegfA, which attenuates Notch signalling by downregulating *notch* gene expression in the arteries. Notch in turn activates the expression of arterial markers such as *ephrinB2* [6, 7]. Thus, identification of other regulators in this process will enhance our understanding of arterial venous differentiation and could provide novel therapeutic targets.

It has been well established that VEGFA gradient formation and signalling is in part regulated by the endothelial glycocalyx component heparan sulphate (HS) proteoglycans [8–11]. HS is synthesised in the golgi as an alternating polymer of *N*-acetyl glucosamine (GlcNAc) and glucuronic acid residues (GlcA). The glycosaminoglycan chain (GAG) undergoes partial deacetylation, N-sulfation, epimerization and O-sulfation. Regulation of biological processes by HS proteoglycans is achieved mainly through eliciting distinct sulfation patterns. In particular the 6-O sulfation patterns have shown to be integral to the activity of many HS binding proteins. The final level of 6-O sulfation is primarily dictated by the action of the recently identified 6-*O* endosulfatases (sulfs) that act to remove sulfate groups both extracellularly and intracellularly [12] thereby controlling the final level of 6-O sulfation pattern within the HS ligand binding sites [13]. The function of SULFs are essential to the activity of many growth factors and morphogens including VEGFA and Hedgehog (Hh), regulating growth factor signaling pathways either at the cell surface or in the extracellular matrix through modulating HS-ligand receptor interaction. Depending on the nature of the 6-*O* sulfated epitope within the HS-bound ligand, SULFs can positively or negatively regulate several signaling pathways during development. For example ectopic *SULF1* expression inhibits VEGFA and FGF mediated angiogenesis by reducing their efficacy for binding to co-receptors [14, 15], but simultaneously can enhance the activity of morphogens such Hh and BMP by facilitating their release from bound receptors or inhibitors to promote formation of a morphogen gradient and consequently generating a signaling response [16, 17]. Conversely loss of *SULF1* increases 6-O sulfation, promoting VEGFA and FGF angiogenic mediated signaling in vitro [14] and reducing Hh signaling [16], suggesting that a controlled level of 6-O sulfation is critical to most signaling pathways. However the role of *sulf1* during vascular development in vivo has not yet been investigated.

In this report, use of transparent, rapidly developing zebrafish larvae has facilitated detailed analysis of the zebrafish homolog of mammalian *sulf1* during vascular development. Embryos lacking *sulf1* expression had arterial malformations in cranial and trunk vasculature concurrent with a switch from arterial to increased venous caudal marker expression. The axial vessel defects were rescued by $vegfa_{165}$ expression, suggesting that sulf1 acts on the VegfA mediated arterial venous differentiation pathway. This was further corroborated by knockdown of *SULF1* by siRNA in HUVECs that led to reduced expression of VEGFA mediated upregulation of arterial markers, strengthening the notion of the role of a HS-editing enzyme *sulf1* in arterio-venous identity.

Methods

Zebrafish stocks

Embryos from transgenic lines Tg(*fli1*:GFP) [18], Tg(*kdrl*:GFP) [19], Tg(*gata-1*:dsRed) [20] and double transgenic tg(*kdrl*:GFP;*gata-1*:dsRed) were raised under standard conditions at 28 °C and staged as described [21]. Embryo media was supplemented with 0.003 % 1-phenyl-2-thiourea after 24hpf to prevent melanin formation [22].

Isolating zebrafish *Sulf1* cDNA

Sulf1, identified on chromosome 24 by an *Ensembl* blast search of human *SULF1* gene against the *Danio rerio* genome, was cloned into $pCS2^{+}$. The deduced amino acid sequence of *Sulf1* (Acc nu:NM_0010023846) was aligned with *Mus musculus* and *Homo sapiens* SULF1 using Clustalw alignment software 2.0. Structural features of the zebrafish Sulf1 protein were predicted using P*fam* [23].

RT-PCR

RNA was extracted from wild type/morphant embryos (20–30 per group) by sonication in trizol, according to manufacturer's instructions, and cleaned up using RNeasy kit (Invitrogen). cDNA synthesis was carried out in 20 µl using 1 µg of RNA, 20 U of AMV reverse transcriptase. PCR was performed in 50 µl, with 1.5 mM $MgCl_2$, and 10 pmol of primers. Primers for *sulf1* expression were *sulf1 fwd*: 5′-TGTCTTCCAGGA GCAGTGTG3′; *sulf1 rev*: 5′-GAGCTTGCCATGAAGGTG AC-3′. Primers used to detect intronic region of *sulf1* transcript were *intron3 fwd2*: 5′-CCAGGTAAAGTGTAGCTATGGC AAA-3′; *exon4 rev2*: 5′-GGACGTCCGCAAATAGTTGA-3′; *β-actin fwd*: 5′-CCTCCGGTCGTA CCACTGGTA T-3′; *β-actin rev*: 5′-CAACGGAAGGTCTCATTGCCGATCGTG-3′. Experiments were done in triplicates.

Whole-mount in situ hybridisation (WISH)

A *sulf1* in situ probe was designed against the 5′UTR region, which is distinct within the sulf homologs. The 511 bp cDNA fragment was amplified with primers *(forward*: 5′-CCCACGATACAGACCTCGTT-3′; *reverse:*5′-GAGCTTTGCTGTCCACTTCC-3′), TA cloned into pGEMT vector (Promega, Madison) and sequenced. WISH was carried out as described in Jowett and Lettice [24] and embryos imaged in 80 % glycerol.

Morpholino knockdown of *sulf1* and rescue experiments

Antisense morpholinos (Gene Tools, Corvallis OR) S1-ATG (5′-CACCAGCTGCATCATGGGACTGCGA-3′) and S1-S B (5′-GTAGTCCTGGTAGTGGTAGAATAAT-3′) were designed against the 5-ATG start codon and predicted splice acceptor site at the end of exon 3 respectively, with mismatch S1-CMO (5′CACgAGgTGgATCATcGGACTcC GA-3′) as a control. 4–5 ng of morpholino with 0.01 % of phenol red was routinely injected in 1–4 cell embryos. For rescue experiments, embryos were co-injected with 50 pg of *sulf1* mRNA cloned into $pCS2^+$ and linearized with *Apa*I. Similarly $vegfa_{165}$ and mutant $vegfa_{165}$ were cloned into $pCS2^+$ and linearised with *not1* and all three transcripts were polymerised by Sp6 RNA polymerase (Ambion, Austin, TX).

Microangiography

Red fluorescent carboxylate modified microspheres 0.02 µm (Invitrogen) were microinjected into the sinus venosus/cardinal vein of zebrafish embryos at 50hpf as described by Isogai et al. [25].

Fluorescent microscopy

Embryos mounted using 3 % methylcellulose or low melting point agarose for long term imaging were photographed using a Zeiss Stereolumar V12 with Axiovision software version 4.6 or a Zeiss LSM 510 META confocal laser microscope using Zeiss LSM software.

Extraction and SAX-HPLC analysis of HS disaccharides

HS was extracted from zebrafish larvae and the disaccharide composition analysed by HPLC with post-column derivitisation, as described by Chen et al. [11]. However, in this instance a Pro-Pac PA1 SAX column (Dionex) was used with a linear gradient of sodium chloride (0–1 M over 70 min). Peaks were identified and peak areas determined by reference to standards of known concentration (0.16nmoles) separated under the same run conditions.

VEGFA stimulation of transfected HUVEC primary cultures

Human umbilical vein endothelial Cells (HUVEC) were isolated from fresh human umbilical cords and cultured in M199 medium (Invitrogen), supplemented with 10 % foetal calf serum (FCS) and endothelial cell growth factor supplement (BD Biosciences) containing heparin (Sigma). HUVECs were transfected with stealth siRNA (Invitrogen) targeting SULF1 (Sequence 1: *Forward* 5′GACUACUU CACAGACUUAAUCACUA-3′, *Reverse* 5′-UAGUGAU UAAGUCUGUGAAGUAGUC-3′; Sequence 2: *Forward* 5′-UGGAAAGAGGCAAAUUUCUACGUAA-3′, *Reverse* 5′-UUACGUAGAAAUUUGCCUCUUUCCA-3′; Sequence 3: *Forward* 5′-AAGAGAUUGAAGCUCUGCAAGAUA A-3′, *Reverse* 5′-UUAUCUUGCAGAGCUUCAAUCUC UU-3′) using lipofectamin RNAi Maxi (Invitrogen) for 4 h before culturing cells in normal growth conditions for 24 h.

Transfected HUVECs were then serum starved in 2 % FCS containing M199 media overnight before being stimulated with VEGFA (25 ng/ml; Invitrogen) for 16 h. RNA was then extracted and qPCR was carried out to determine changes in gene expression of SULF1 (*Forward*: 5′-ACCA GACAGCCTGTGAACAA-3′, *Reverse*: 5′-ATTCGAAGC TTGCCAGATGT-3′), *DLL4* (*Forward*: 5′-CCCTGGCAAT GTACTTGTGAT-3′, *Reverse*: 5′-TGGTGGGTGCAGTAG TTGAG-3′) and *HEY11* (*Forward*: 5′-CGAGCTGGACGA GCCCAT-3′, *Reverse*: 5′-GGAACCTAGAGCCGAACTC A-3′) relative to *GAPDH* (*Forward*: 5′-AGCCACATCGC TCAGACAC-3′, *Reverse*: 5′-GCCCAATACGACCAAAT CC-3′).

Results

Identification and cloning of the zebrafish *sulf1* gene

Genomic database mining identified three extracellular zebrafish Sulfs, two *HSULF-2* paralogs and one ortholog of *HSULF-1*, '*zsulf1*', the focus of this paper. The zebrafish *sulf1* locus is syntenic with the human chromosomal location 8q13.2, harbouring the human *SULF1* gene. The predicted full length of the transcript is 4.6 kb (Ensembl Accession number ENSDART00000027022) and was cloned from 24hpf larvae RNA. The predicted amino acid sequence (Ensembl zebrafish assembly version 7.0, Sanger Institute, Cambridge, UK) shows 73 % identity to human and murine SULF1. It encodes a putative 874 amino acid protein organised into four conserved domains: N-terminal, enzymatic domain, hydrophilic and C-terminal (Fig S1). The enzymatic sulfatase domain is highly conserved and features the cysteine residue critical for hydrolytic cleavage of the sulfate group from the substrate [26, 27]. The asparagine linked glycosylation sites (important in heparin binding) are also conserved [28].

Temporal and spatial expression of *sulf1*

From our previous studies on *sulf1* expression we found maternally derived *sulf1* transcripts were present in fertilized zebrafish embryos (1hpf) and zygotic *sulf1* was expressed during gastrulation and somitogenesis, but downregulated at 48hpf [29]. Spatial expression of *sulf1* was examined by WISH from 50 % epiboly to 60hpf (Fig S2). Expression was detectable in the developing axial vessels (AVs), the eye, presumptive midbrain/hindbrain structures, floorplate of the spinal cord and somite boundaries (SBs). By 24hpf strong expression was maintained in these regions as well as in the heart, branchial arches and caudal vascular plexus. Interestingly expression of *sulf1* in the caudal plexus coincided with a period of active angiogenesis in this region, as confirmed by *kdrl* expression, a marker for endothelial cells. At 48hpf, *sulf1* expression was confined to distinct regions of the head including the eye and primordial hindbrain channel (PHBC) of the cranial vasculature, in addition to being maintained in the AVs and pronephric ducts.

Morpholino knockdown of *sulf1* mRNA

To assess the functional role of *sulf1* in zebrafish vascular development, we injected embryos separately with two antisense morpholinos, a translation blocker (S1-ATGMO) and a splice blocker (S1-SBMO). Both induced reproducible morphological abnormalities at 26-72hpf (Fig. 1a–i). At 26hpf, 63 % of *sulf1* 5 ng S1-ATGMO morphants exhibited a "characteristic" phenotype with caudal oedema (Fig. 1b black arrow) and a mild depression in the hindbrain (indicated by length of black line in Fig. 1b compared to 1a). At 60hpf, the majority of these morphants displayed pericardial oedema and blood pooling in the mid region of the tail (Fig. 1d, black arrows). By 72hpf, blood pooling in the head and tail was present in 50 % of morphants, indicative of vascular related defects (Fig. 1f–h black arrows). These phenotypes were not seen in embryos injected with a 5 bp mismatch control morpholino (CMO) (Fig. 1i). Despite the circulatory defects the heart rate was normal in morphants. A small subset (8 %) of 'moderate' *sulf1* morphants, where the vascular phenotype was complicated by a ventrally curved body axis (Fig S3), were excluded from further analysis. Results from here on refer to the characteristic phenotype class of *sulf1* morphants.

The specificity of the characteristic phenotype in the S1-SBMO morphants, was confirmed by RT-PCR and sequencing (Fig S4 and data not shown). The S1-SBMO was predicted to eliminate exon4 in the enzymatic domain of the *sulf1* transcript. Although we detected reduced levels of *sulf1* wildtype mRNA transcript until 48hpf (Fig S4B), at the optimum morpholino dose of 5 ng, no *sulf* transcript lacking exon4 (523 bp) was detected. However using a second primer set spanning intron3 and exon4 we detected increased levels of a truncated *sulf1* transcript encoding exon3 spliced to a portion of intron3 and exon4, (Fig S4B, S1 Intron transcript). This is similar to intron inclusions seen for other splice blocking morpholinos [30]. Thus the predicted intron in the final *sulf1* transcript would produce a shift in the reading frame resulting in the introduction of a premature stop codon at the beginning of the intron3 sequence, hypothetically rendering translation of a truncated Sulf1 protein. In addition 15–20 % of published morpholinos exhibit off-target effects mediated through the activation of the apoptotic p53-dependent pathway, including characteristic small head and eyes [31, 32]. The S1-ATGMO defects were reproducible in the $p53^{-/-}$ embryos [33], suggesting the effects are not mediated by p53 (data not shown).

sulf1 morphants show an increase in 6-O sulfation

Previous reports show that sulfatases act at the cell surface to remove 6-*O* sulfate groups from tri-sulfated(UA2S GlcNS6S), di-(UAGlcNS6S) and mono-sulfated (UAGlcNAc6S) disaccharides of HS chains [34, 35]. To confirm that S1-ATGMO affected HS sulfation in vivo, HS from 48hpf wildtypes, control morphants and *sulf1* morphants was digested into disaccharides and analysed by HPLC. The six main HS disaccharides identified by comparison to standards included the three 6-*O*-sulfated disaccharides (Fig. 2a peaks 3, 4 and 6). Significant increases were observed in the *N*- and 6-*O*-sulfated disaccharide 'UAGlcNS6S' (peak 4, 34 %) and the tri-sulfated disaccharide 'UA2SGlcNS6S' (peak 6, 24 %)

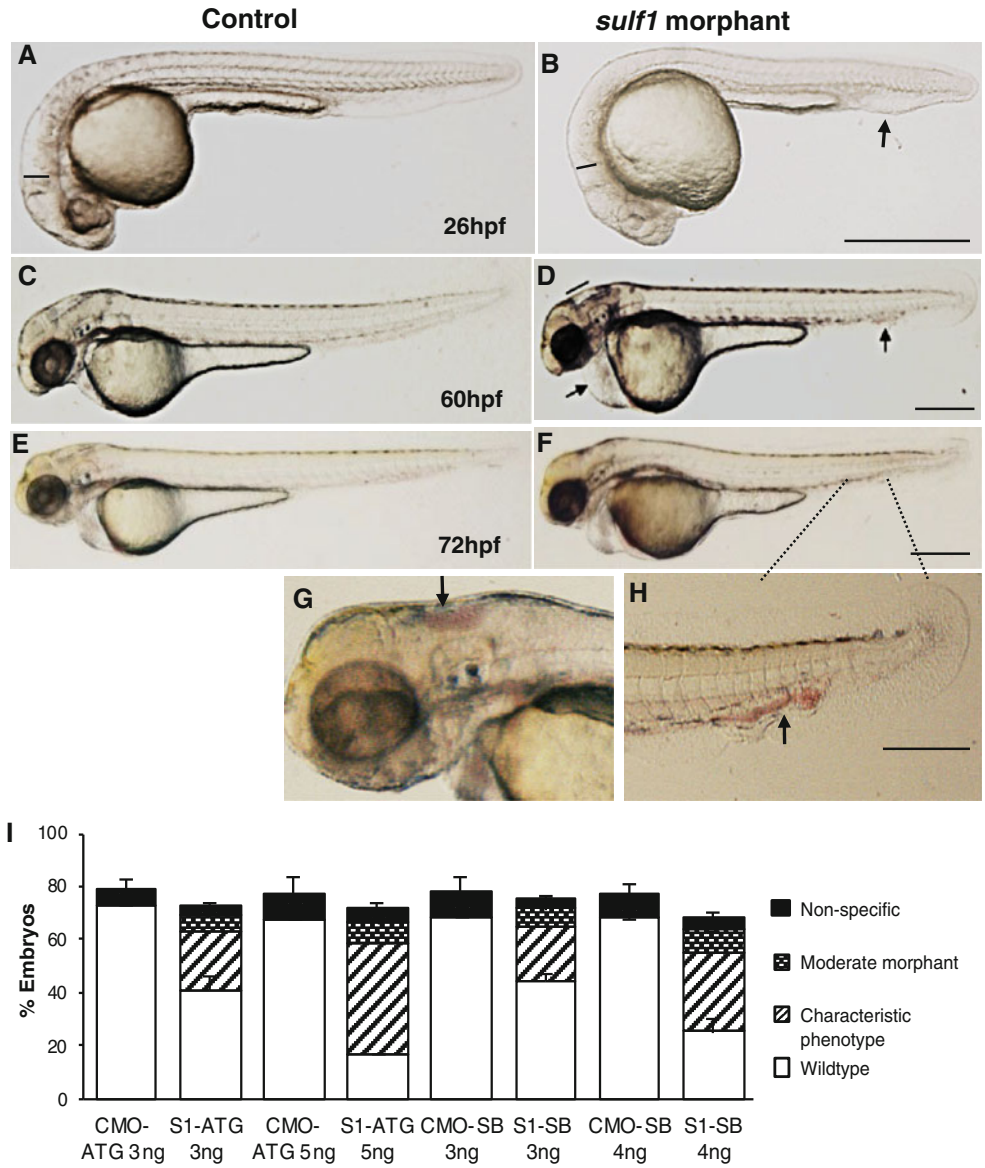

Fig. 1 Characteristic morphology of *sulf1* morphants. Brightfield images of tg(*kdrl*:GFP;*gata-1*:dsRed) embryos injected with control S1-CMO (**a**, **c**, **e**) and S1-ATGMO, (**b**, **d**, **f**, **g**, **h**). The black lines indicate mild depression in the hindbrain of morphants and black arrow in tail and head depict vascular oedema and haemorrhage respectively. Scale bar of images **a**–**h**; 500 μm. Percentage of embryos displaying the characteristic phenotype (**i**), (n = 4 experiments each of 70–80 embryos). Error bars indicate SE

in the morphant embryos compared to controls, with a concomitant decrease of the di-sulfated disaccharide 'UA2SGlcNS' (peak 5, Fig. 2b). These findings are consistent with mice and quail SULF1 activities [34–36] and the total level of change in 6-O sulfation is comparable with that of previous studies with *hs6st2* knockdown in zebrafish [11, 37].

sulf1 morphants display circulatory defects

To determine the precise onset of the circulatory defects i.e. pooling of blood in the tail and head, morphants were analysed at four different time points in the tg(*gata-1*:dsRed) line. At 26hpf axial circulation appeared normal in wildtype and *sulf1* morphant embryos (Fig S5A-B) with blood flowing down the dorsal aorta (DA/CA) from the anterior trunk to the tail, and connecting with the posterior cardinal vein (PCV/CV) to return blood to the heart and the rest of the embryo. At 35hpf, *sulf1* morphants (S1-ATGMO and S1-SBMO) retained the arterial-venous connection formed at 26hpf (Fig. 3b, red arrow), leading to the formation of a premature arteriovenous shunt (A-V shunt) and as a result prevented the blood from circulating in the caudal artery (CA) and the tail caudal plexus (Fig. 3b red bracket). Consistently, the position of the A-V shunt always resided at the 18th somite from the rostral end. In spite of the aberrant A-V connection in the *sulf1* morphants, blood flow began to be

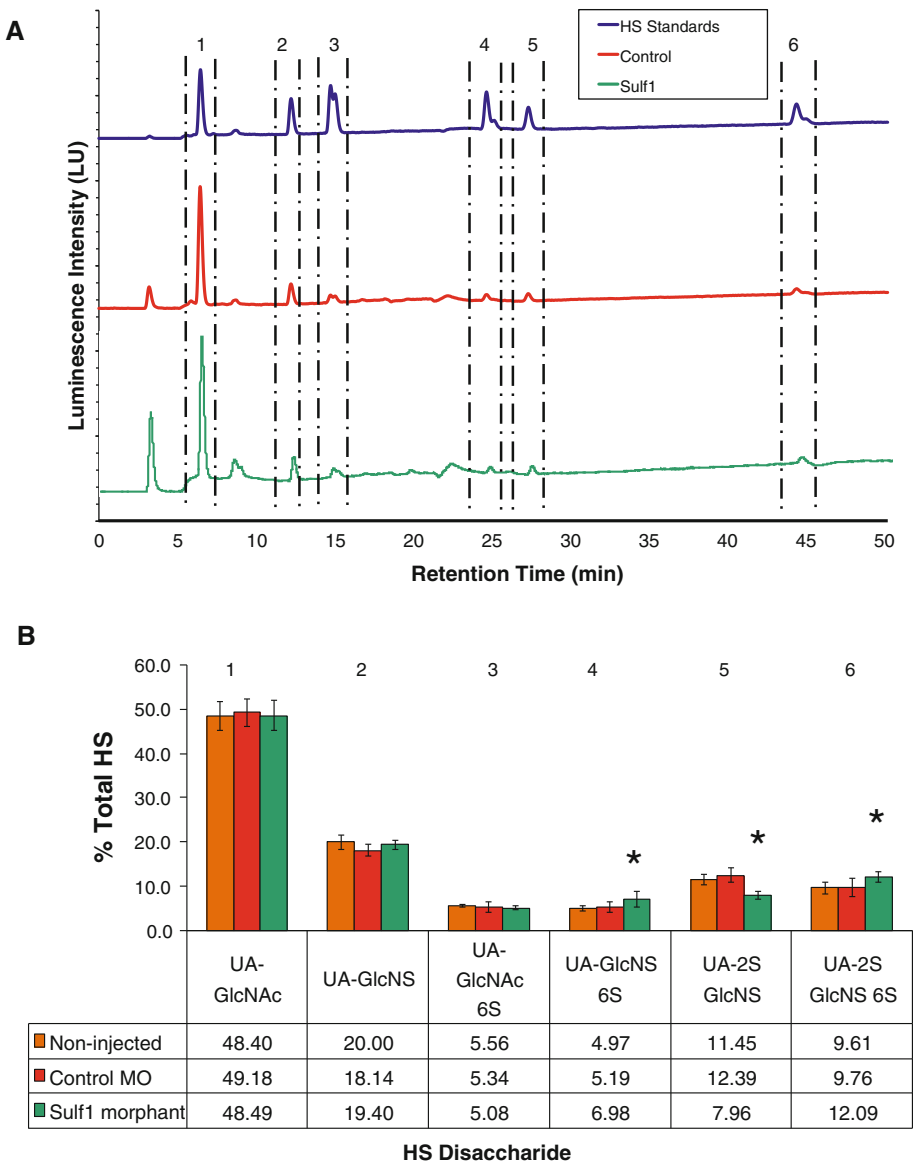

	UA-GlcNAc	UA-GlcNS	UA-GlcNAc 6S	UA-GlcNS 6S	UA-2S GlcNS	UA-2S GlcNS 6S
Non-injected	48.40	20.00	5.56	4.97	11.45	9.61
Control MO	49.18	18.14	5.34	5.19	12.39	9.76
Sulf1 morphant	48.49	19.40	5.08	6.98	7.96	12.09

Fig. 2 *sulf1* knockdown increases HS 6-O-sulfation. A representative chromatogram of SAX-HPLC disaccharide analysis of HS from the wildtype, S1-CMO and 5 ng *sulf1* injected embryos (**a**). Six disaccharides were identified by comparison to the elution times of known HS standard peaks; *peak 1*: Δ4,5 unsaturated hexuronate-*N*-acetyl glucosamine (ΔUA-GlcNAc); *peak 2*: ΔUA-*N*-sulfated glucosamine, (ΔUA-GlcNS); *peak 3*: ΔUA-6-*O*-sulfated GlcNAc (ΔUA-GlcNAc6S); *peak 4*: ΔUA-6-*O*-sulfated GlcNS, (ΔUA-GlcNS6S); *peak 5*: ΔUA2-*O*-sulfated GlcNS (ΔUA2S-GlcNS); *peak 6*: ΔUA2S-GlcNS6S. **b** Disaccharide analysis of HS extracted from 48hpf wildtype, control MO injected, and *sulf1* morphant embryos. *Asterisk* denotes significant changes in the disaccharide compared to control injected embryos. Standard deviation calculated from 5 individual experiments (n = 5) 40–60 embryos per experiment (T test $p < 0.05$)

rerouted to the end of the tail by 48hpf (Fig. 3d red arrowhead). This became more apparent at 72hpf when blood circulation could be observed unevenly in the caudal plexus, posterior to the A-V shunt (Fig. 3f, red bracket). The route of the blood circulation to the tail was from the functioning intersegmental vessels (ISVs) connected to the caudal plexus (Fig. 3f, red arrow) as opposed to the caudal artery, where no blood flow was observed immediately posterior to the A-V shunt. Furthermore, the normal remodelling of the caudal plexus to a single ventral tube at 72hpf [25, 38] failed to occur in the morphants, as displayed by the asymmetrical blood circulation in the tail, compared to that of the control (Fig. 3e, f).

Early cranial circulation detected at 26hpf in control injected and *sulf1* morphants (Fig S5A, B) was indistinguishable, but at 35hpf *sulf1* morphants did not exhibit the strong cranial circulation (Fig. 3b, white arrows) as observed in the control injected embryos (Fig. 3a). At 48hpf *sulf1* morphants, began to show circulation in the main arterial cranial route i.e. lateral dorsal aortae (LDA) and posterior hindbrain channel (PHBC), but there was little or no circulation penetrating the forebrain and midbrain (Fig. 3d, red bracket). By 72hpf, very weak or no circulation was evident in the central arteries (CtA) encompassing the hindbrain (Fig. 3h, white asterisks). A schematic dorsal view of the cranial vasculature is also shown, recapitulating the regions of reduced (grey) or no (black) cranial circulation in hindbrain of *sulf1* morphants (Fig. 3j). In addition other vascular structures such as the subintestinal vessels and pharyngeal arches/arteries also lacked blood circulation (Fig S5D, red asterisks).

Both axial and cranial circulatory defects were consistent with both morpholinos (Fig. 4a, b), 94 and 95 % of the S1-SBMO and S1-ATGMO *sulf1* morphants respectively,

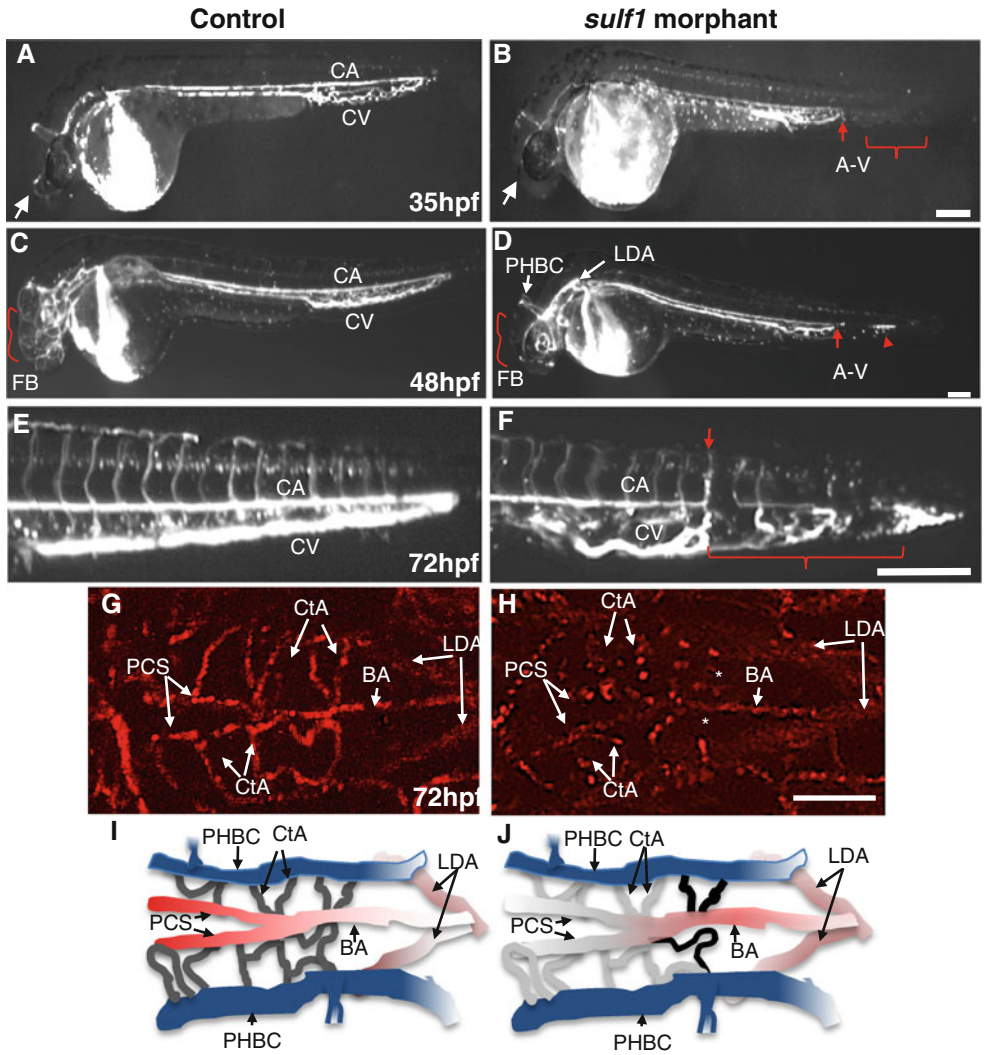

Fig. 3 *sulf1* morphants exhibit circulatory defects, **a**–**d**; Fluorescent digital stereoimages of live blood flow in tg(*gata-1:*dsRed). At 35hpf *sulf1* morphants (**b**) display A-V shunt (*red arrow*) with no circulation in the forebrain compared to control (*white arrow*). By 48hpf *sulf1* morphants (**d**) show little or no circulation in the tail, posterior to the A-V shunt (*red arrow*) and mid-forebrain regions (*red bracket*). The presence of blood in the caudal tail (*red arrowhead*) suggest some functional circulation. The aberrant blood circulation continues at 72hpf (**f**) with axial blood flow re-routing to the caudal tail via the intersegmental arteries (ISA) (A-V, *red arrow*) and caudal vein displaying irregular blood flow (*red bracket*). A dorsal view of cranial circulation in the *sulf1* morphant (**h**) showing reduced overall circulation in the head with no circulation in central arteries (CtA) marked by white asterisk. A schematic illustration of the cranial circulation defect in *sulf1* morphants (**j**) compared to control (**i**), reduced circulation is depicted by the grey colored areas. CtA colored in black denote missing circulation. *Scale bar* 200 μm (**a**–**f**) and 100 μm (**g**, **h**). *A-V* arteriovenous shunt, *BA* basilar artery, *CA* caudal artery, *CtA* central arteries, *CV* caudal vein, *FB* forebrain, *LDA* lateral dorsal aorta, *PCS* posterior communicating segment, *PHBC* primodial hindbrain channel

displayed an A-V shunt at 72hpf which was absent in control injected embryos (Fig. 4a). Reduced cranial circulation was evident in 86 % of S1-SBMO and 93 % of S1-ATGMO *sulf1* morphants, of which 35 % of S1-SBMO and 51 % of S1-ATGMO morphants (Fig. 4b) developed cranial haemorrhages. To confirm that the phenotype was specific for *sulf1*, we co-injected S1-SBMO with full length zebrafish *sulf1* mRNA to rescue the circulatory defects present in *sulf1* morphants. In three independent experiments, analysis of the morphants at 72hpf showed a significant rescue of the phenotype with 77 % of embryos retaining normal axial and cranial circulation (one way ANOVA $p < 0.05$) (Fig. 4c).

sulf1 morphants display defects in vascular patterning and integrity

To determine the cause of the circulatory defects, the vascular patterning of *sulf1* morphants was examined by confocal microscopy in tg(*kdrl*:GFP;*gata-1*:dsRed) embryos. At 12hpf

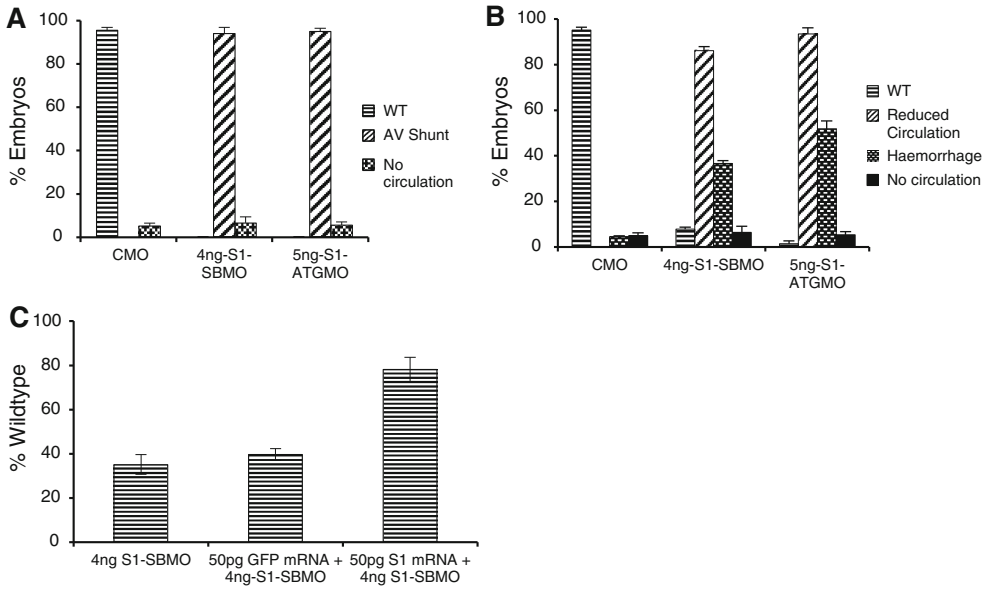

Fig. 4 *sulf1* circulatory defects can be rescued with *sulf1* mRNA. Quantification of number of 72hpf *sulf1* morphants with defects in axial circulation (**a**), and in cranial circulation (**b**), (N = 4, 70–80 embryos per experiment). Rescue experiment (**c**) displaying the total percentage of embryos with normal axial and cranial circulation after injection of 50 pg *sulf1* mRNA with S1-SBMO, (N = 3, 65–70 embryos per experiment). *Error bars* indicate SE, **one way *ANOVA* $p < 0.05$ versus S1-SBMO alone

sulf1 morphants showed *kdrl*$^{+}$ endothelial cells migrating from the lateral plate mesoderm into the ventral midline, indicating normal endothelial cell specification (data not shown). At 26hpf there was a clear demarcation of the CA and CV vessels in the control injected embryos (Fig. 5a). In a starked contrast, the endothelial cells of the CV, in the *sulf1* morphant, aggregated to the region of the growing caudal artery (Fig. 5b, white arrowhead) resulting in a failed demarcation of the CA and CV boundaries posterior to the A-V shunt (Fig. 5b, white bracket). The precise position of this vascular defect coincided with the A-V shunt observed in the injected tg(*gata-1*:ds-Red) embryos. By 48hpf, the aberrant development of the CA and CV was evident in *sulf1* morphants, thus a visibly small and thin lumenised CA (Fig. 5d, f white arrowhead) maintained the premature connection to CV (Fig. 5f, white arrow) i.e. the A-V shunt. The CV was not clearly demarcated in the morphants, with a mass of endothelial cells posterior to the A-V shunt that did not coalesce to form a branched vasculature network in the caudal plexus (Fig. 5c, d, white bracket). As a result, blood could be observed pooling in the extravascular tissue of the *sulf1* morphants (Fig S5F, white arrowhead). A schematic illustration of the caudal tail is also shown as a representative of the *sulf1* morphant exhibiting a smaller caudal artery at the site of the A-V shunt (Fig. 5h). The accumulation of endothelial cells in the CV at the site of the A-V shunt led us to hypothesize that an 'overproliferation' of endothelial cells was resulting in a block/termination of the caudal artery. To test this possibility we measured the number of proliferative endothelial cells in the tail of the *sulf1* morphant from 26 to 48hpf by staining with anti-phosphohistone (anti-PH3) and quantifying the number of cells in the caudal plexus. However we found no significant difference in the number of proliferating cells (data not shown).

Analysis of the cranial vasculature indicated normal patterning of the primary vessels such as PHBC, basilar artery (BA) and mesencephalic vein (MsV) in *sulf1* morphants at 26hpf (data not shown). At 48hpf there are a specific number of cranial vessels that are formed via angiogenesis during development. One specific group of cranial vessels is the CtA's that sprout from the PHBC and circulate blood to the BA and PCS. In the *sulf1* morphant several CtA formed thin endothelial cord like structures, and connected to the BA but remained non-functional, as evident by the lack of blood flow (Fig. 5j, white arrows), thus suggesting a failure of the vessels to lumenise correctly. Evidently most posterior CtA were absent or did not form connections (Fig. 5j white asterisk), such defects are likely to be responsible for the oedema and haemorrhage that ensue in these areas of the head (Fig S5H, inset). As further confirmation of the loss of vascular integrity (i.e. vessel leakiness and lack of a patent lumen in some vessels), we performed microangiography using red fluorescent microspheres in *sulf1* morphants. Functional circulation was observed in 48hpf wildtype (Fig S6), whilst in *sulf1* morphants circulation did not progress into the most caudal region of the tail and was diverted through an A-V shunt (Fig S6B, white arrow). Anterior to the trunk, fluorescent microspheres could be observed 'leaking' into mesodermal tissue surrounding the cranial vasculature of

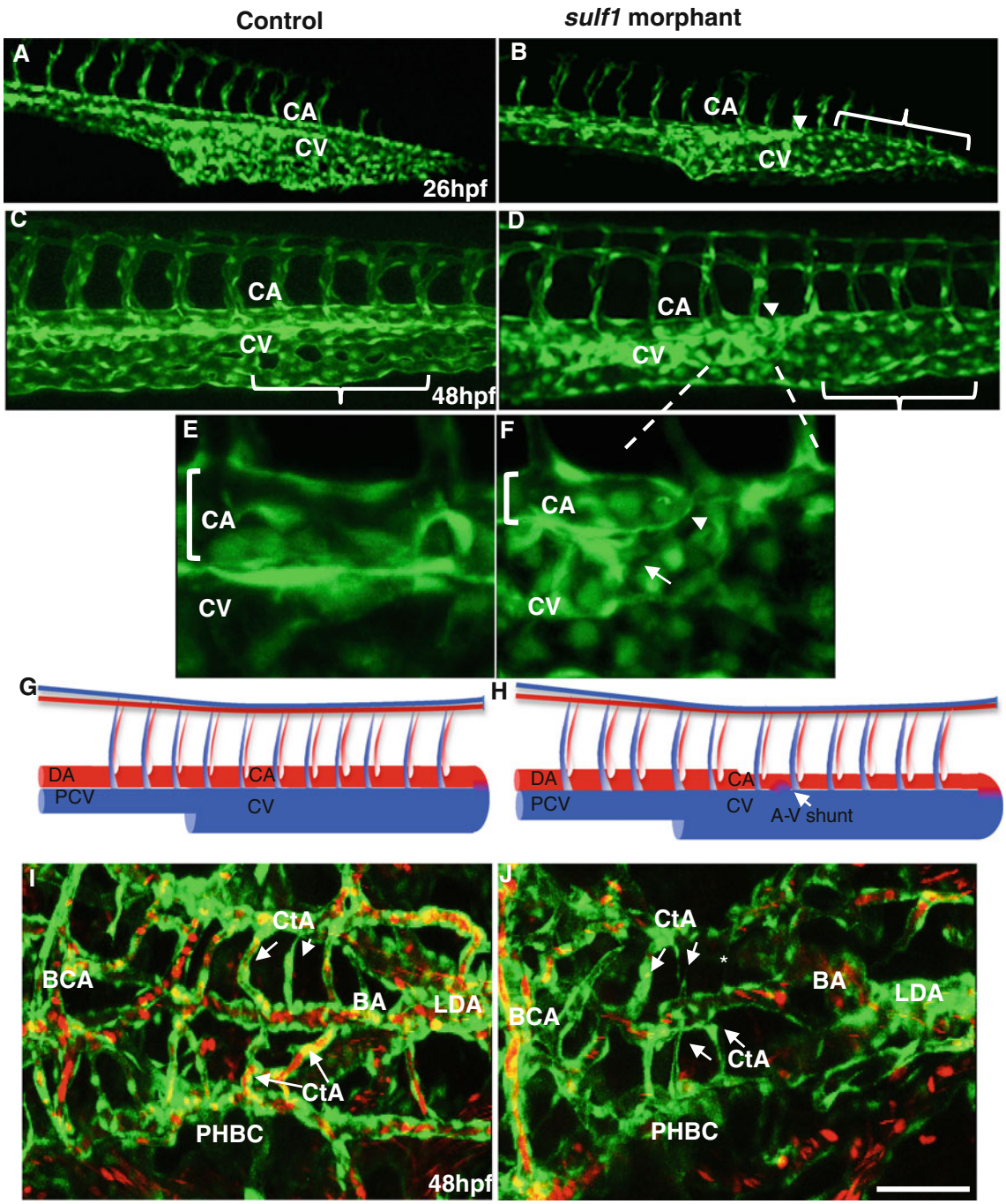

Fig. 5 *sulf1* knockdown results in impaired vessel formation at the site of circulatory defect. Confocal microscopic analysis of the vasculature in tg(*kdrl:*GFP;*gata-1:*dsRed) *sulf1* morphants. **a**–**h** Lateral views of the trunk, caudal to the right. Developing tail vasculature in 26hpf control (**a**) and *sulf1* morphant (**b**) showing a less developed CA (*white arrowhead*). At 48hpf the caudal plexus (denoted by *white bracket*) in the *sulf1* morphant (**d**) is highly disorganised with no clear vascular lumenisation compared to control (**c**). Higher magnification of the caudal artery defect in the *sulf1* morphant (**f**) shows abrupt termination of a very thin CA (*white arrowhead*) and the premature CA connection to CV (*white arrow*). A schematic illustration of the trunk vasculature in *sulf1* morphants (**h**), highlighting the aberrant A-V connection and the narrowing of the CA. Dorsal view of cranial vasculature, in control (**i**) and morphants. The *sulf1* morphant (**j**) show "ropey like" central arteries that are not lumenised (*white arrows*) as indicated by the lack of blood flow. *BA* basilar artery, *BCA* basilar communicating artery, *CA* caudal artery, *CtA* central arteries, *DA* dorsal aorta, *LDA* lateral dorsal aorta, *PA* pharyngeal arches, *PHBC* primordial hindbrain channel. *Scale bar* 50 μm

the hindbrain (Fig S6D). This was consistent with previous circulatory defects noted in the tg(*fli & kdrl*:GFP;*gata-1*:dsRed) *sulf1* morphants and further corroborated the vasculature defects.

sulf1 morphants lack arterial gene expression in a localised region of the caudal tail

To elucidate the cellular basis of the caudal artery defect, we next analysed expression of several endothelial markers by WISH in control and *sulf1* morphants at 24hpf. No differences in the expression pattern of the pan-endothelial marker *kdrl* (*vegfA receptor 2*) was detected in *sulf1* morphants compared to control (Fig. 6a, b), suggesting normal angioblast differentiation, proliferation, migration and coalescence at the midline. The DA, PCV and ISV development were correctly initiated, consistent with our initial observations of the vasculature in Tg(*kdrl*:GFP;*gata-1*:dsRed) embryos. To test whether *sulf1* plays a role in endothelial cell differentiation into arterial or venous cells, *sulf1* morphants were analysed for expression of arterial markers such as *notch3*, *deltaC*, *ephrinB2*, *sox7* and *sox18*. Although no changes in *sox7* and *sox18* expression were detected when compared to control embryos *(data not shown)*, the *sulf1* morphants showed a specific loss of *notch3*, *deltaC* and *ephrinB2* arterial marker expression at the 18th somite from the rostral end corresponding to the A-V shunt of the CA (Fig. 6d, f, h, compare to Fig. 6c, e, g), whilst neural expression of these markers remained unaffected (Fig S7). Examination of the markers of venous cell fate *flt4* (*vegfA* receptor 3), *dab2* and *stab 2* in *sulf1* morphants in the same region (Fig. 6j, l, n) showed clear ectopic expression in the CA (red bar) in addition to their normal expression in the caudal vein (CV, black bar). Quantitative measurements of the region were taken by measuring the width of in situ staining from caudal vein to caudal artery. *sulf1* morphants showed a 27 %, statistically significant increase in *flt4* venous marker in this region of the tail (average of 45.4 μm in controls versus 57.7 μm in *sulf1* morphants, $n = 14$, $p \leq 0.01$) suggesting there was an increased expression of *flt4* in CA cells compared to controls. The venous marker expression was expanded at the expense of arterial expression, consistent with the development of a small CA and aberrant demarcation of the CA and CV boundaries. This led us to hypothesise *sulf1* has a role in specifying arterial-venous identity.

Ectopic $vegfa_{165}$ mRNA restores normal circulation in sulf1 morphants

$VEGFA_{165}$ is one of several heparin-binding growth factors that play an essential role during vasculogenesis. One of the roles of $VegfA_{165}$ during early vascular development is to direct differentiation of angioblasts in the lateral mesoderm to an arterial or venous fate. The somitic expression of $vegfa_{165}$ regulates the arterial differentiation of the first *kdrl* angioblasts migrating toward the midline by activation of the notch signaling pathway [6]. To assess if Sulf1 was acting on the VegfA pathway, we co-injected 2 pg of $vegfa_{165}$ mRNA and *sulf1* ATGMO to see if we could rescue the aberrant axial and cranial circulation in *sulf1* morphants. To control for any non-specific effects, we used $vegfa_{165}$ mRNA that had a mutation in the receptor tyrosine kinase domain. $Vegfa_{165}$ mRNA doses were carefully titrated to a dose that alone elicited only minimal effects on vascular development (data not shown). Co-injected embryos were analyzed at 35hpf and 48hpf for axial and cranial circulation and the percentage of embryos showing wildtype like circulation was scored (Fig. 7). *Sulf1* morphants co-injected with $vegfa_{165}$ showed a statistically significant increase ($\sim$50 %) in wildtype axial circulation and an increase of 31 % in wildtype cranial circulation. However higher concentrations of $vegfa_{165}$ did not rescue cranial circulation any further (data not shown).

To further elucidate the cellular basis of the CtA defect in the head we analyzed the expression of markers for vasculature integrity *tie2*, *ve-cad*, *ang-1* and $vegfa_{165}$ in *sulf1* morphants by WISH, prior to onset of the secondary cranial vessel formation (Fig S8). No difference was observed in *tie2* and *ve-cad* expression in the head of the *sulf1* morphants (Fig S8B,D), but weaker $vegfa_{165}$ and *ang-1* expression was evident in the mid-forebrain of the morphants compared to wildtype (Fig S8F,I,J, L black arrows). At 28hpf $vegfa_{165}$ expression was reduced in the mid-forebrain regions of morphants in comparison to control injected embryos (Fig S8M-N). This suggested that *sulf1* is required for proper $vegfa_{165}$ expression in the head and consequently for cranial vessel maturation.

SULF1 is essential for upregulation of arterial markers by VEGFA in vitro

As VEGFA is critical for arterial specification both in vitro and in vivo [6] we next examined whether *SULF1* knockdown affected VEGFA mediated arterial venous specification by measuring the direct effect of VEGFA mediated upregulation on arterial markers *HEY1* and *DLL4* in human umbilical vascular endothelial cells (HUVECs) by qPCR. Incubation of HUVECs with VEGFA for 16 h induced a 14-fold increase in *DLL4* expression, which was decreased over 60 % by knockdown of *SULF1* with 3 separate siRNAs targeted to *SULF1* (Fig. 8a). Similarly, VEGFA-stimulated *HEY1*expression was reduced over 70 % by *SULF1* siRNAs, (Fig. 8b). Interestingly VEGFA also stimulated *SULF1* expression (Fig. 8c) and this facilitated confirmation that each of the siRNAs was able to

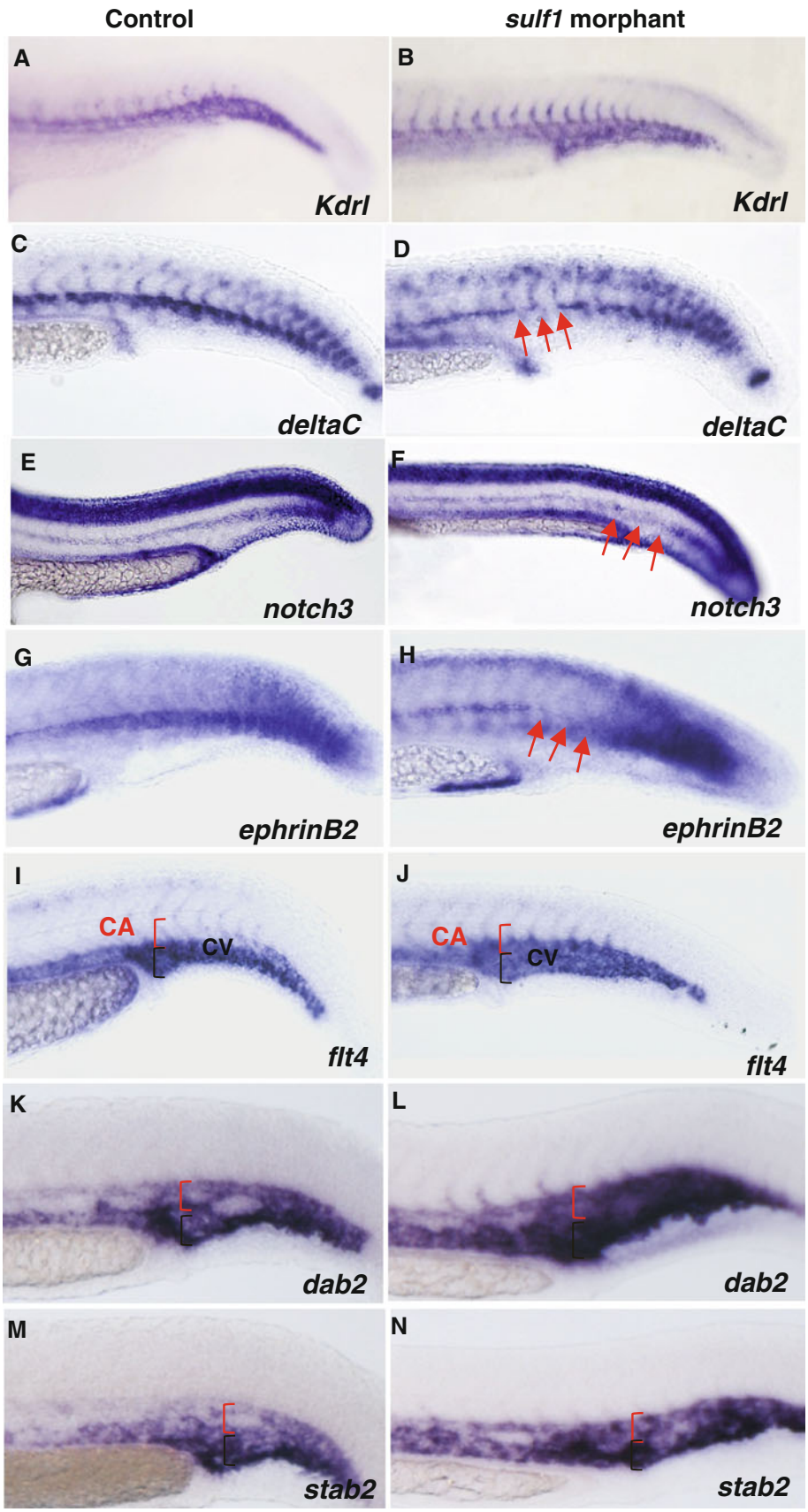

Fig. 6 Control injected embryos and *sulf1* morphants were analysed at 24hpf for the expression of the indicated arterial and venous markers by WISH (**a**–**n**). Lateral views of the whole tail are shown. *sulf1* morphants (**d**, **f**, **h**) display lack of expression of arterial markers *deltaC* (**d** 16 out of 21 embryos examined), *notch3* (**f**; 18 out of 24 embryos examined) and *ephrinB2a* (**h**; 11 out of 15 embryos examined) shown by *red arrows*. In contrast *sulf1* morphants display an expansion of the venous markers in the caudal artery indicated by *red bar* (**j**, **l**, **n**) compared to control. *flt4* (**j**; 19 out of 24 embryos examined) *dab2* (**l**) and *stab 2* (**n**). *CA* caudal artery, *CV* caudal vein

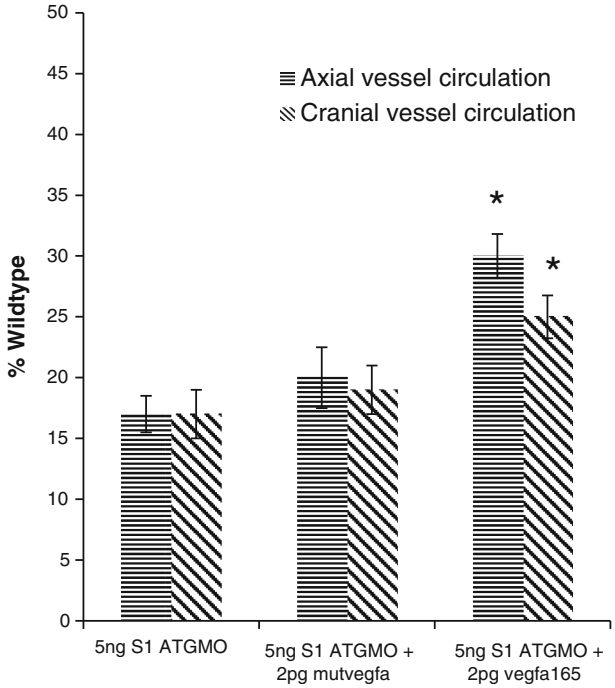

Fig. 7 *vegfa*$_{165}$ mRNA restores normal circulation in *sulf1* morphants. Rescue experiment displaying the total percentage of embryos with normal axial and cranial circulation after injection of 2 pg *vegfa*$_{165}$ mRNA with S1-ATGMO, versus S1-ATGMO alone (N = 5, 80 embryos per experiment). *Error bars* indicate SE, *asterisk* one way *ANOVA* $p < 0.05$

knock down VEGFA stimulated *SULF1* expression by 75 %. This suggests a possible feedforward loop, which could further explain the significant percentage of *sulf1* morphants that develop normal axial and cranial circulation when co-injected with *vegfa*$_{165}$ mRNA. These results further corroborate that knockdown of *sulf1* affects Vegfa$_{165}$ mediated arterial venous identity.

Discussion

Enormous structural diversity on HS proteoglycans is created by HS modifying enzymes, forming unique binding sites for growth factors critical to the development of a functional circulatory system. HS 6-*O*-sulfotransferases (HS6STs) and sulfatases create a specific 6-O sulfation pattern of HS essential for vessel formation both in vitro and in vivo. Evidence for this has been shown in HS6ST1$^{-/-}$ mice that die at birth [39] partly due to vascular complications and in zebrafish *hs6st2* morphants that exhibit largely defects in angiogenesis [11]. In this report we propose a novel functional role for zebrafish *sulf1* in vascular development.

In zebrafish, *sulf1* knockdown results in mild morphological defects in the head and tail of the morphants with malformation of the axial vessels. The fact that a stronger

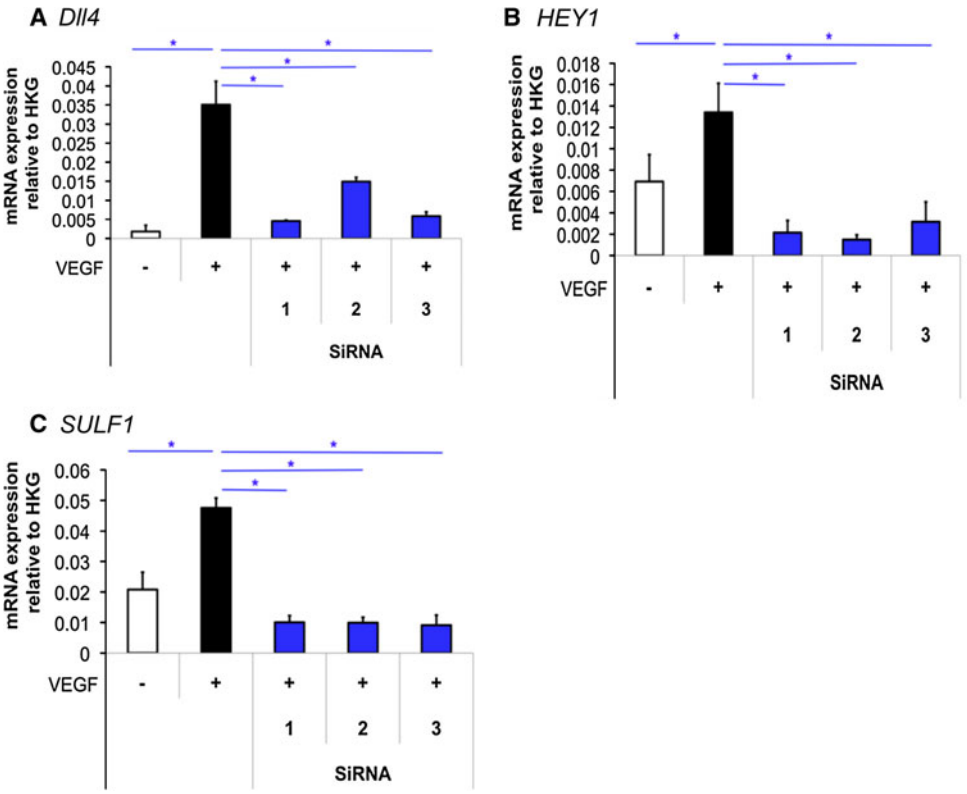

Fig. 8 *SULF1* knockdown abrogates *Dll4* and *HEY1* induction in response to VEGFA stimulation in HUVECs. HUVEC stimulated with VEGFA (25 ng/ml) for 16 h up-regulated the expression of *Dll4* (**a**), *HEY1* (**b**) and *SULF1* (**c**). This induction was significantly reduced following knockdown of *SULF1* expression by three independent siRNAs in HUVECs. *$p < 0.001$, unpaired student *t* test. *Error Bars* SD

and earlier vascular phenotype was not observed in early stages of vascular development suggests that there may be functional compensation by other Sulf enzymes from neighbouring tissues. Consistent with this idea, all three *sulfs* are ubiquitously expressed during early embryonic vascular development. However, during mid somitogenesis when arterial venous cell differentiation takes place (15ss–17ss) *sulf1* is preferentially expressed in the axial vasculature and expands into the cranial vasculature at later stages (2dpf). The fact that the *sulf1* morphant harbors a single A-V shunt where only a subset of arterial cells has switched to venous cell identity hints at the presence of some residual wildtype Sulf1 protein. Furthermore, strong expression of *sulf2a* and *sulf2* in neighbouring tissues of the vasculature, mostly residing in the nervous system could explain why distinct regions of cranial vasculature are affected [29]. This hypothesis is further corroborated by HS disaccharide analysis in *sulf1* morphants, where only a modest increase in HS 6-O sulfation is observed and the fact that knocking down multiple sulfs arrested development prior to vasculogenesis (data not shown). Mouse *SULF1* and *SULF2* show similar functionally redundant roles in skeletal development [40].

sulf1 morphants displayed a vestigial A-V shunt and impaired cranial circulation which could be rescued by overexpressing *sulf1* mRNA. In the head, a subset of immaturely formed secondary cranial vessels (CtA) was observed, which was further confirmed by microangiography. Haemorrhage in these morphants appeared to be a consequence of the immature vasculature. Although formation of the vascular tube is correctly initiated, the incorrect specification of a number of arterial cells as venous cells could contribute to the occlusion of the caudal aorta leading to the aberrant A-V shunt. Similar vascular defects have been described in mutants or morphants of the VegfA, Notch and Sox7/Sox18 pathway that display arterial-venous malformations leading to circulatory defects in the DA, ISVs and cranial vessels [7, 41–48].

In zebrafish, arterial identity is controlled by Shh from the notochord/hypochord inducing $vegfa_{165}$ expression in the somites which upregulates *notch3* expression in the presumptive arterial cells. Notch3 is critical for arterial maturation of the DA as it downregulates the venous marker *flt4* expression and activates the arterial marker *ephrinB2a* in arterial cells [7]. Sox7 and Sox18 have also been shown to regulate arterial venous identity [46–48]. *sox7* expression is thought to be regulated by Vegf signalling pathway [48]. *sox7* when synergistically knocked down with *sox18* also results in A-V shunt and arterial venous identity defects similar to that of the *sulf1* morphants. Although *sox7/sox18* morphants resembled the *sulf1* morphant phenotype, we did not observe a difference in *sox7/sox18* expression in *sulf1* morphants, suggesting *sox7/sox18* is functioning independently of the Vegf signaling pathway.

Interestingly, there was a noticeable lack of expression of other arterial markers *ephrinB2a*, *notch3* and *deltaC* and an increase of the venous markers *flt4*, *dab2* and *stab 2* in the CA of the *sulf1* morphants suggesting that the CA is "mis-programmed" and that *sulf1* is required for arterial identity and maturation of the CA. Since *tie2* expression was unaffected, this confirmed the loss of arterial marker expression rather than a loss of endothelial cell identity.

The *sulf1* morphant phenotype resembled the loss of arterial identity seen in *kdrl/flk1*, *plcγ1*(phospholipase C gamma-1, a downstream effector of VegfA, and *mindbomb (notch)* mutants [7, 41, 42], further evidence that notch signalling in arterial differentiation is modulated by the VegfA pathway [6]. The lack of an intersegmental artery phenotype in *sulf1* morphants, which was seen in the *plc-γ1* and *mindbomb* mutants, can be attributed to the compensatory effects of co-expression of *sulf2a* in the somite boundaries, but not in the caudal aorta [29]. *In vitro* studies have shown that 6-O desulfation of HS by sulfatases has a significant role in modulating $VEGFA_{165}$ activity [14] and that 6-*O* sulfate groups are critical for HS to bind to $VEGFA_{165}$ [49]. It is possible that the over 6-*O*-sulfated HS formed in *sulf1* morphants may not facilitate the appropriate interaction of $VegfA_{165}$ with its receptors, retaining $VegfA_{165}$ in the ECM or cell surface. Similarly in mice the VEGF splice variant which binds HS most tightly, $VEGFA_{188}$, was defective in supporting arterial development [50]. Ectopic expression of $vegfa_{165}$ rescued the aberrant circulation, supporting the notion that Sulf1 can modulate $VegfA_{165}$ activity in vivo. Our in vitro data further confirmed that *SULF1* knockdown reduces the effects of VEGFA on arterial gene expression in endothelial cells, consistent with a role for *sulf1* in arterial venous identity in the developing aorta. In HUVECs there appears to be a feed-forward mechanism to enhance the effects of VEGFA by induction of *SULF1*, since lack of this induction reduces expression of notch signalling components *DLL4* and *HEY1*, indicating sulf1 as a novel component of the VegfA mediated arterial specification pathway. We hypothesize that during early vascular development when arterial and venous cells are being specified, Vegf signaling at the endothelial cell surface or in the extracellular matrix is regulated spatially and temporally by Sulf1. An increase in HS-6-O sulfation interferes with $VegfA_{165}$ interacting with its receptors, leading to a subset of endothelial cells that differentiate as venous cells instead of arterial cells. This occurs in a temporally and spatially specific manner reflecting where Sulf1 is unavailable. During arterial and venous cell migration the mispositioning of the "venous cells" in the caudal artery leads to the formation of a premature A-V shunt.

In conclusion, this study provides the first in vivo evidence that the HS-modifying gene *sulf1* plays a role in arterial venous identity, vascular patterning and arterial integrity. Subtle changes in the sulfate moieties of HS brought about by morpholino mediated knockdown of *sulf1* had specifically localised defects, as may be anticipated by the strict developmental regulation of HS enzymes. These results strengthen the notion that the finely balanced 6-O sulfation pattern provided by Sulf enzymes are critical to control HS mediated physiological processes. Our findings that *sulf1* affects arterial venous identity and maturation indicates that it may be of therapeutic interest in HTT and in therapeutic angiogenesis.

Acknowledgments We would like to thank the BSU staff at the Universities of Manchester and Oxford for taking care of the aquarium and the staff at the confocal microscope core facilities. This work was funded by University of Manchester Medical School strategic studentship, British Heart Foundation, Diabetes UK, Medical Research Council and Cancer Research UK. Conceived and designed the experiments: BG and SS. Performed the experiments: BG, FL, EB, RM Analyzed the data: BG, FL, EB, SS. Contributed reagents/materials/analysis tools: FL, AS, KLK, RP, AH, TC, XM. Wrote the paper: BG and SS with input from RP and AH authors.

Conflict of interest There are no conflicts of interest.

References

1. Adams RH, Klein R (2000) Eph receptors and ephrin ligands: essential mediators of vascular development. Trends Cardiovasc Med 10(5):183–188
2. Hirashima M, Suda T (2006) Differentiation of arterial and venous endothelial cells and vascular morphogenesis. Endothelium 13(2):137–145
3. Irrthum A et al (2003) Mutations in the transcription factor gene *SOX18* underlie recessive and dominant forms of hypotrichosis-lymphedema-telangiectasia. Am J Hum Genet 72(6):1470–1478
4. Carmeliet P et al (1996) Abnormal blood vessel development and lethality in embryos lacking a single VEGF allele. Nature 380(6573):435–439
5. Olsson AK et al (2006) VEGF receptor signalling—in control of vascular function. Nat Rev Mol Cell Biol 7(5):359–371
6. Lawson ND, Vogel AM, Weinstein BM (2002) Sonic hedgehog and vascular endothelial growth factor act upstream of the Notch pathway during arterial endothelial differentiation. Dev Cell 3(1):127–136
7. Lawson ND et al (2001) Notch signalling is required for arterial-venous differentiation during embryonic vascular development. Development 128(19):3675–3683
8. Ashikari-Hada S et al (2005) Heparin regulates vascular endothelial growth factor(165)-dependent mitogenic activity, tube formation, and its receptor phosphorylation of human endothelial cells—comparison of the effects of heparin and modified heparins. J Biol Chem 280(36):31508
9. Jakobsson L et al (2006) Heparan sulfate in *trans* potentiates VEGFR-mediated angiogenesis. Dev Cell 10(5):625–634
10. Ruhrberg C et al (2002) Spatially restricted patterning cues provided by heparin-binding VEGF-A control blood vessel branching morphogenesis. Genes Dev 16(20):2684–2698
11. Chen E et al (2005) A unique role for 6-O sulfation modification in zebrafish vascular development. Dev Biol 284(2):364–376
12. Frese MA, Milz F, Dick M, Lamanna WC, Dierks T (2009) Characterization of the human sulfatase Sulf1 and its high affinity heparin/heparan sulfate interaction domain. J Biol Chem 284: 28033–28044
13. Gorsi B, Stringer SE (2007) Tinkering with heparan sulfate sulfation to steer development. Trends Cell Biol 17(4):173–177
14. Narita K et al (2006) HSulf-1 inhibits angiogenesis and tumorigenesis in vivo. Cancer Res 66(12):6025–6032
15. Wang S et al (2004) QSulf1, a heparan sulfate 6-O-endosulfatase, inhibits fibroblast growth factor signaling in mesoderm induction and angiogenesis. Proc Natl Acad Sci USA 101(14):4833–4838
16. Kleinschmit A et al (2010) Drosophila heparan sulfate 6-O endosulfatase regulates Wingless morphogen gradient formation. Dev Biol 345(2):204–214
17. Viviano BL et al (2004) Domain-specific modification of heparan sulfate by Qsulf1 modulates the binding of the bone morphogenetic protein antagonist Noggin. J Biol Chem 279(7):5604–5611
18. Lawson ND, Weinstein BM (2002) In vivo imaging of embryonic vascular development using transgenic zebrafish. Dev Biol 248(2):307–318
19. Jin SW et al (2005) Cellular and molecular analyses of vascular tube and lumen formation in zebrafish. Development 132(23):5199–5209
20. Traver D et al (2003) Transplantation and in vivo imaging of multilineage engraftment in zebrafish bloodless mutants. Nat Immunol 4(12):1238–1246
21. Kimmel CB et al (1995) Stages of embryonic development of the zebrafish. Dev Dyn 203(3):253–310
22. Westerfield M et al (1997) An on-line database for zebrafish development and genetics research. Semin Cell Dev Biol 8(5): 477–488
23. Bateman A et al (2000) The Pfam protein families database. Nucleic Acids Res 28(1):263–266
24. Jowett T, Lettice L (1994) Whole-mount in situ hybridizations on zebrafish embryos using a mixture of digoxigenin- and fluorescein-labelled probes. Trends Genet 10(3):73–74
25. Isogai S, Horiguchi M, Weinstein BM (2001) The vascular anatomy of the developing zebrafish: an atlas of embryonic and early larval development. Dev Biol 230(2):278–301
26. Dierks T et al (1999) Sequence determinants directing conversion of cysteine to formylglycine in eukaryotic sulfatases. EMBO J 18(8):2084–2091
27. von Figura K et al (1998) A novel protein modification generating an aldehyde group in sulfatases: its role in catalysis and disease. BioEssays 20(6):505–510
28. Ambasta RK, Ai X, Emerson CP Jr (2007) Quail Sulf1 function requires asparagine-linked glycosylation. J Biol Chem 282(47): 34492–34499
29. Gorsi B, Whelan S, Stringer SE (2010) Dynamic expression patterns of 6-O endosulfatases during zebrafish development suggest a subfunctionalisation event for sulf2. Dev Dyn 239(12):3312–3323
30. Morcos PA (2007) Achieving targeted and quantifiable alteration of mRNA splicing with Morpholino oligos. Biochem Biophys Res Commun 358(2):521–527
31. Ekker SC, Larson JD (2001) Morphant technology in model developmental systems. Genesis 30(3):89–93
32. Robu ME et al (2007) p53 activation by knockdown technologies. PLoS Genet 3(5):e78
33. Berghmans T et al (2005) Prognostic role of p53 in stage III non-small cell lung cancer. Anticancer Res 25(3c):2385–2389
34. Ai X et al (2007) SULF1 and SULF2 regulate heparan sulfate-mediated GDNF signaling for esophageal innervation. Development 134(18):3327–3338

35. Lamanna WC et al (2006) Heparan sulfate 6-O-endosulfatases: discrete in vivo activities and functional co-operativity. Biochem J 400(1):63–73
36. Ai X et al (2006) Substrate specificity and domain functions of extracellular heparan sulfate 6-O-endosulfatases, QSulf1 and QSulf2. J Biol Chem 281(8):4969–4976
37. Bink RJ et al (2003) Heparan sulfate 6-o-sulfotransferase is essential for muscle development in zebrafish. J Biol Chem 278(33):31118–31127
38. Huang CC et al (2003) reg6 is required for branching morphogenesis during blood vessel regeneration in zebrafish caudal fins. Dev Biol 264(1):263–274
39. Habuchi H et al (2007) Mice deficient in heparan sulfate 6-O-sulfotransferase-1 exhibit defective heparan sulfate biosynthesis, abnormal placentation, and late embryonic lethality. J Biol Chem 282(21):15578–15588
40. Ratzka A et al (2008) Redundant function of the heparan sulfate 6-O-endosulfatases Sulf1 and Sulf2 during skeletal development. Dev Dyn 237(2):339–353
41. Covassin LD et al (2009) A genetic screen for vascular mutants in zebrafish reveals dynamic roles for Vegf/Plcg1 signaling during artery development. Dev Biol 329(2):212–226
42. Covassin LD et al (2006) Distinct genetic interactions between multiple Vegf receptors are required for development of different blood vessel types in zebrafish. Proc Natl Acad Sci USA 103(17):6554–6559
43. Lawson ND et al (2003) Phospholipase C gamma-1 is required downstream of vascular endothelial growth factor during arterial development. Genes Dev 17(11):1346–1351
44. Nasevicius A, Larson J, Ekker SC (2000) Distinct requirements for zebrafish angiogenesis revealed by a VEGF-A morphant. Yeast 17(4):294–301
45. Ober EA et al (2004) Vegfc is required for vascular development and endoderm morphogenesis in zebrafish. EMBO Rep 5(1): 78–84
46. Cermenati S et al (2008) Sox18 and Sox7 play redundant roles in vascular development. Blood 111(5):2657–2666
47. Herpers R et al (2008) Redundant roles for sox7 and sox18 in arteriovenous specification in zebrafish. Circ Res 102(1):12–15
48. Pendeville H et al (2008) Zebrafish Sox7 and Sox18 function together to control arterial-venous identity. Dev Biol 317(2): 405–416
49. Robinson CJ et al (2006) VEGF165-binding sites within heparan sulfate encompass two highly sulfated domains and can be liberated by K5 lyase. J Biol Chem 281(3):1731–1740
50. Stalmans I et al (2002) Arteriolar and venular patterning in retinas of mice selectively expressing VEGF isoforms. J Clin Invest 109(3):327–336